Cell Death and Differentiation (2009) 16, 498–511

www.nature.com/cdd

Inhibition of Aurora B kinase sensitizes a subset of human glioma cells to TRAIL concomitant with induction of TRAIL-R2

J Li[1], MG Anderson[2], LA Tucker[1], Y Shen[1], KB Glaser[1] and OJ Shah*[,1]

Small-molecule inhibitors of the Aurora A and B kinases interfere with mitotic centrosome function and disrupt the mitotic spindle assembly checkpoint resulting in polyploidization and apoptosis of proliferating cells. As such, several Aurora kinase inhibitors are at various stages of clinical development as anticancer agents. To identify candidate apoptosis-sensitizing genes that could be exploited in combination with Aurora kinase inhibitors in malignant glioma, we have carried out global gene expression analysis in a D54MG glioma cell derivative treated with three Aurora kinase inhibitors chosen for their distinctive selectivities: MLN8054 (Aurora A-selective), AZD1152 (Aurora B-selective), and VX-680 (Aurora A/B). The modulation of apoptotic gene expression by p53 under these conditions was ascertained, as p53 expression can be toggled on and off in this D54MG derivative by virtue of a stable, inducible, p53-targeting short hairpin RNA (D54MG^{shp53}). This analysis identified the tumor necrosis factor-related apoptosis-inducing ligand (TRAIL) death receptor, TRAIL receptor 2 (TRAIL-R2), as an apoptosis-sensitizing gene induced selectively following inhibition of Aurora B. In glioma cell lines where TRAIL-R2 was induced following polyploidization, the sensitivity, kinetics, and magnitude of TRAIL-mediated apoptosis were enhanced. Our data shed light on the apoptotic program induced during polyploidization and suggest that TRAIL-R2 activation is a putative point of therapeutic intervention in combination with inhibitors of Aurora B.
Cell Death and Differentiation (2009) **16,** 498–511; doi:10.1038/cdd.2008.174; published online 12 December 2008

The Aurora kinase family comprises three structurally related, serine/threonine kinases (Aurora A, B, and C) that serve critical, nonredundant functions during cell division. Aurora A is required for early mitotic events, such as centrosome maturation and separation, mitotic spindle assembly, and chromosome congression to the metaphase plate.[1] Aurora B is an element of the mitotic 'spindle assembly checkpoint,' a safeguard that ensures that chromosome segregation does not proceed until all kinetochores and microtubules are precisely attached. The expression of Aurora C is restricted primarily to the testis where it appears to be involved in meiotic cell division.[2] Collectively, the Aurora kinases represent a novel family of mitotic targets, and small-molecule inhibitors of one or more family members are aggressively being developed as neocytotoxic anticancer agents.

Owing to the distinct functions of Aurora A and B in mitosis, the cytotoxicities induced by Aurora A- or B-selective small-molecule inhibitors are phenotypically unique. MLN8054, an Aurora A-selective inhibitor, produces mitotic spindle assembly deficiencies concomitant with mitotic delay or arrest, whereas at higher concentrations polyploidy (the appearance of >4n DNA content) is observed.[3,4] Both the Aurora B-selective pyrazoloquinazoline, AZD1152,[5,6] and the pan-Aurora inhibitor, VX-680,[7] induce polyploidization, which eventually leads to apoptosis. All three classes of inhibitors are efficacious in multiple human xenograft models validating the Aurora kinases as viable cancer targets.[3,7,8] Nevertheless, how these agents affect cell fate decisions that influence apoptosis is still poorly defined. We have observed, in multiple cancer cell lines, that despite the induction of polyploidy, cells with an apparently normal DNA complement eventually emerge (data not shown). Thus, therapeutic strategies that potentiate apoptosis of polyploid cells may be of clinical utility by enhancing antiproliferative activity and suppressing the emergence of cancer cells that may have undergone significant genetic reshuffling.

Under severe cellular stress, apoptosis is initiated by engaging a complex network of cell-intrinsic and -extrinsic signal transduction pathways. The former involves activation of pro-apoptotic and/or neutralization of anti-apoptotic BH3-containing proteins such that a threshold level of mitochondrial permeablization and caspase activation is achieved. The cell-extrinsic pathway initiates apoptosis from the cell surface through ligand recognition of multimeric transmembrane receptors of the TNF receptor superfamily known as death receptors. Death receptor activation leads to the rapid

[1]Cancer Biology Division, Global Pharmaceutical Research and Development, Abbott Laboratories, Abbott Park, IL 60064-6121, USA and [2]Advanced Technologies, Global Pharmaceutical Research and Development, Abbott Laboratories, Abbott Park, IL 60064-6121, USA
*Corresponding author: OJ Shah, Cancer Biology Division, R47J, Abbott Laboratories, 100 Abbott Park Road, Building AP9, Room 2169, Abbott Park, IL 60064-6121, USA. Tel.: 847 937 2745; Fax: 84 793 536 22; E-mail: jameel.shah@abbott.com
Keywords: Aurora A; Aurora B; TRAIL; TRAIL-R2; polyploidization; glioma
Abbreviations: FACS, fluorescence-activated cell sorting; FADD, Fas-associated death domain; IPA, Ingenuity Pathway Analysis; PE, phycoerythrin; shRNA, short hairpin RNA; TRAIL, tumor necrosis factor-related apoptosis-inducing ligand; TRAIL-R1, tumor necrosis factor-related apoptosis-inducing ligand receptor 1; TRAIL-R2, tumor necrosis factor-related apoptosis-inducing ligand receptor 2
Received 25.3.08; revised 26.9.08; accepted 29.9.08; Edited by A Ashkenazi; published online 12.12.08

assembly of the death-inducing signaling complex, comprising the Fas-associated death domain (FADD) adapter protein and pro-caspases 8 and 10. The association with FADD triggers the auto-activation of caspase-8 and -10, which in turn proteolyze and activate the apoptotic effectors caspase-3/-6/-7.

Here we define the global transcriptional response to polyploidization secondary to inhibition of Aurora kinases in a p53-positive human glioma cell line and find that polyploidization results strictly from inhibition of Aurora B. We also define elements of the transcriptional response that are p53 dependent. Furthermore, upregulation of tumor necrosis factor-related apoptosis-inducing ligand receptor 2 (TRAIL-R2) by Aurora B inhibition is concomitant with sensitization of a subset of human glioma cells to TRAIL-mediated apoptosis, although p53 status *per se* is not absolutely correlated with TRAIL sensitization. These data provide a mechanistic rationale for combining Aurora kinase inhibitors with death receptor agonists in the management of glioma.

Results

We rationalized that understanding the mechanisms of Aurora kinase-mediated cell death could reveal particular apoptotic processes that were amenable to therapeutic exploitation. We therefore analyzed the transcriptional response to Aurora kinase inhibition with two key questions in mind: (1) how is Aurora A *versus* Aurora B inhibition differentially reflected in the transcriptional response, and (2) as p53 is known to be induced during polyploidization,[9–11] how does p53 influence the transcriptional response and is this related to Aurora A or Aurora B inhibition *per se*? Using two immunofluorescence assays, we first established the cellular activity of three reference compounds toward Aurora A (mitotic spindle assembly, Figure 1a) and Aurora B (mitotic histone H3 phosphorylation; Figure 1b). Using these data, we defined three Aurora kinase selectivity conditions, each representing the optimal selectivity profile for Aurora A and Aurora B and each exceeding the respective compound's IC_{50}: 250 nM

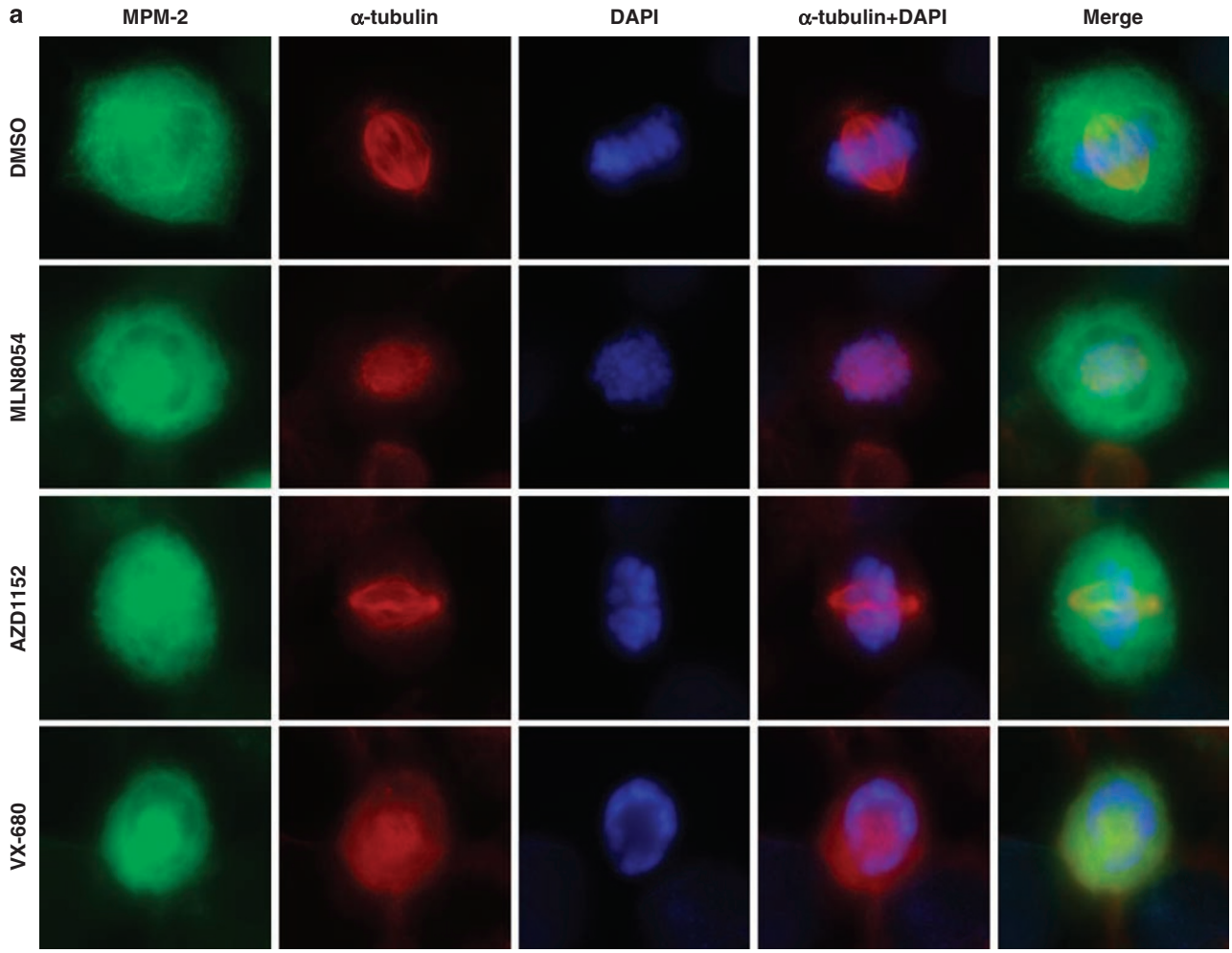

Figure 1 Definition of cellular Aurora A, B, and A/B selectivity conditions. D54MG cells were seeded onto glass coverslips and exposed to MLN8054, AZD1152, or VX-680 in half-log dose response as indicated and cultured for a further 6 h. Cells were fixed and stained with the indicated primary antibodies. Cells were either triple-labeled with anti-MPM-2, anti-α-tubulin, and DAPI (**a**) or double-labeled with anti-MPM-2 and anti-histone H3-(pSer^{10}) (**b**). (**c**) Quantitation of cellular Aurora A and Aurora B activity. Aurora A inhibition was determined by scoring the number of metaphase bipolar spindles (an indirect measurement of mitotic spindle assembly) observed in the mitotic (MPM-2-positive) fraction. Aurora B inhibition was determined by scoring the number of histone H3-(pSer^{10})-positive cells within the mitotic (MPM-2-positive) fraction. For both assays, 50 mitotic cells were scored for each compound concentration. The data are expressed as the percentage of DMSO-treated control cells

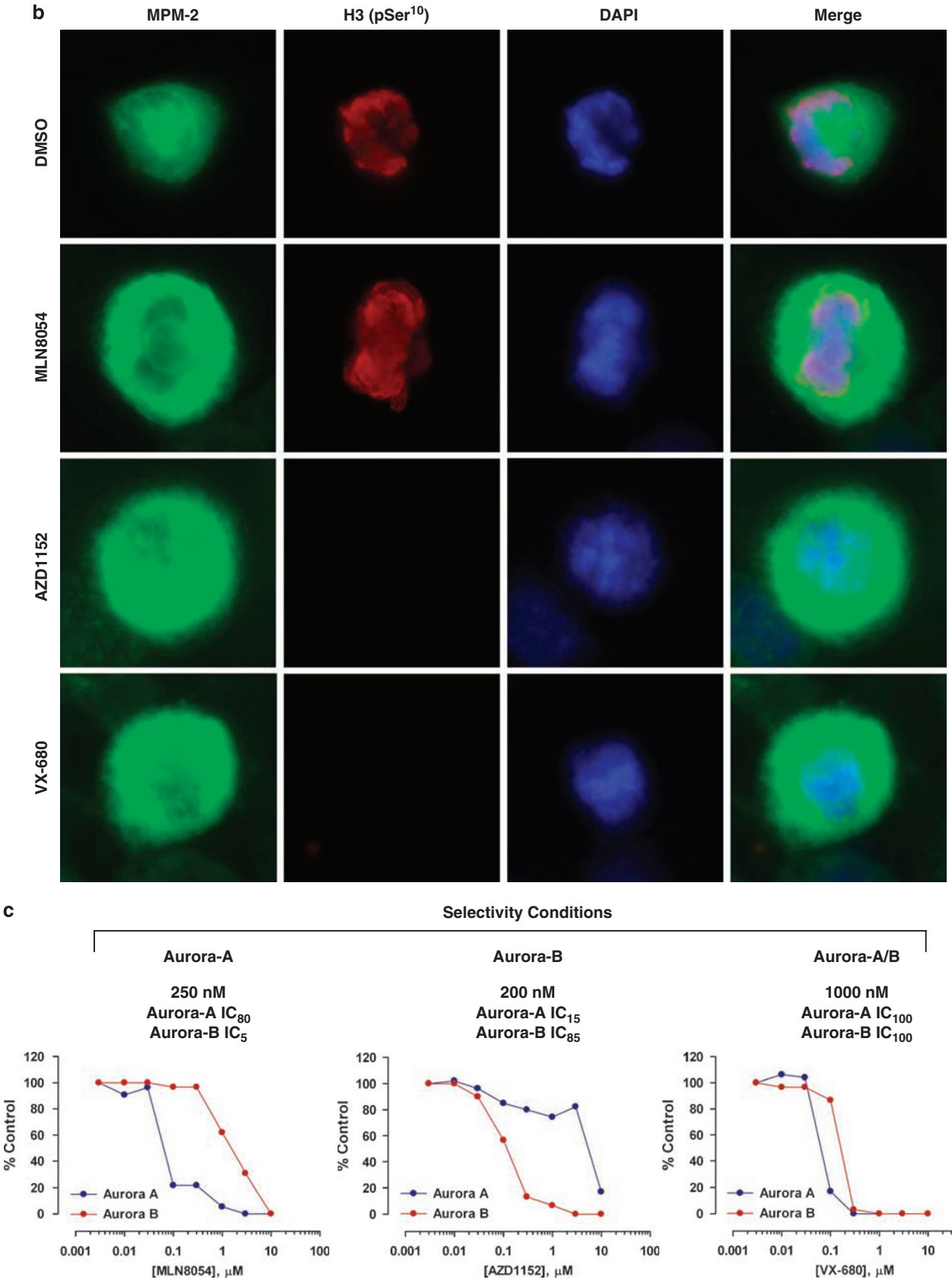

Figure 1 (continued)

MLN8054, Aurora A-selective; 200 nM AZD1152, Aurora B-selective; and 1000 nM VX-680, pan-Aurora A/B (Figure 1c). Fluorescence-activated cell sorting (FACS) analysis indicated that both Aurora B and A/B inhibition elicited polyploidization, as populations with 4n and 8n DNA content accumulated in cells exposed to AZD1152 and VX-680 (Figure 2a and b).

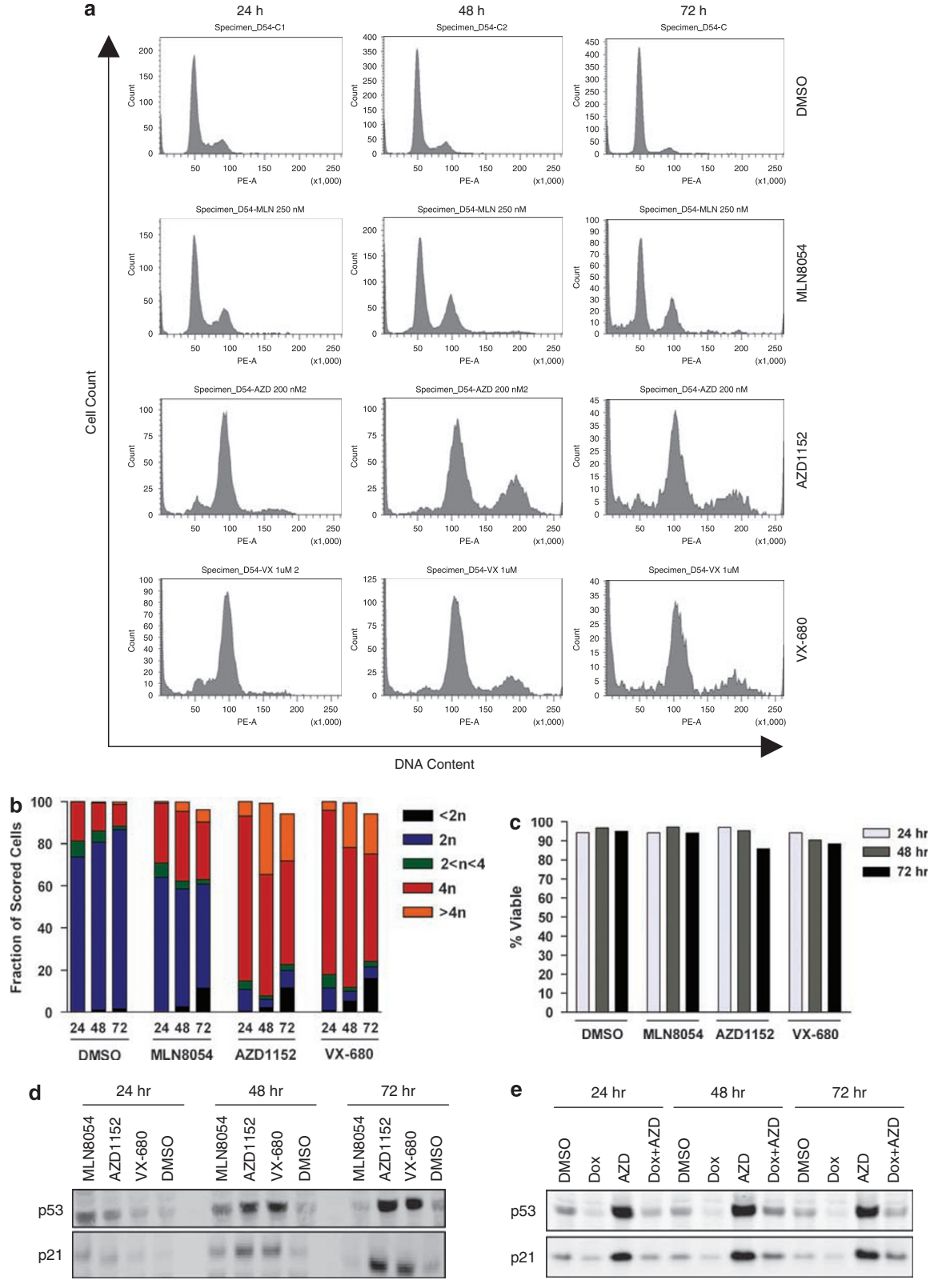

Figure 2 (continued)

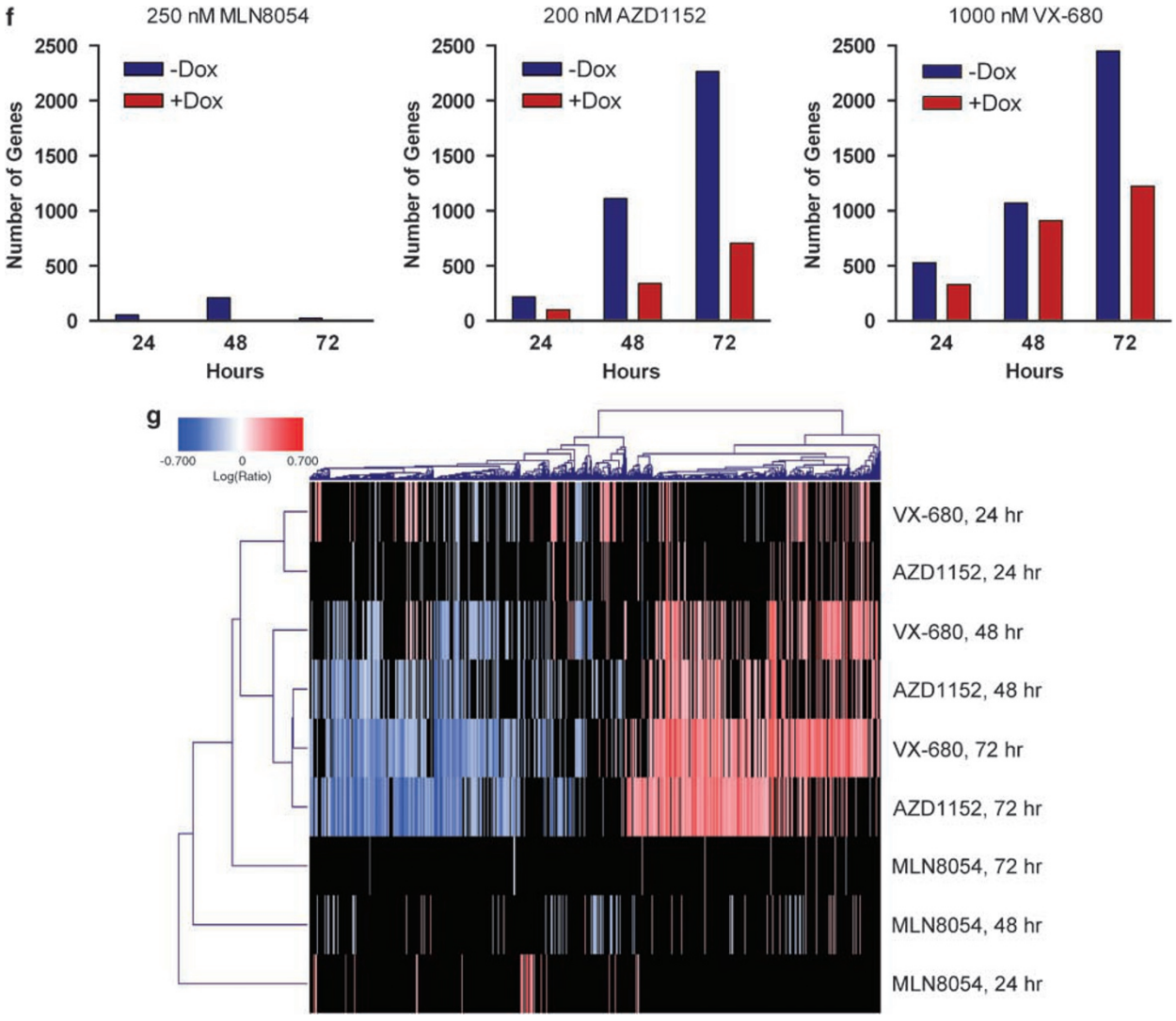

Figure 2 Polyploidization, viability, and transcriptional response to Aurora kinase inhibition. (**a**) D54MG^{shp53} cells were treated with DMSO, 250 nM MLN8054, 200 nM AZD1152, or 1000 nM VX-680 and cultured for a further 24, 48, or 72 h as indicated. Cells were washed, fixed, permeabilized, stained with propidium iodide, and analyzed by flow cytometry for polyploidization and cell death. (**b**) The PI intensities of individual peaks from (**a**) were quantified and expressed. (**c**) D54MG^{shp53} cells were treated as in (**a**) and viability was determined by trypan blue exclusion and quantified using a Vi-Cell cell counter. (**d**) D54MG^{shp53} cells were treated as in (**a**) and cell lysates were prepared. Western analysis of p53 and p21 are shown. (**e**) D54MG^{shp53} cells were treated with 50 ng/ml doxycycline for 24 h before the addition of 200 nM AZD1152 for the times indicated. Cell lysates were then prepared, and p53 and p21 protein expression was determined by immunoblotting. (**f**) Total RNA was prepared from D54MG^{shp53} cells treated first for 24 h with 50 ng/ml doxycycline followed by 250 nM MLN8054, 200 nM AZD1152, or 1000 nM VX-680 for the times indicated. Probe sets whose *P*-values conform to a 5% false-discovery rate and satisfied a secondary filter of 1.5-fold expression change (relative to DMSO-treated cells from the same time point) were counted, indicating total number of significant gene changes. (**g**) Hierarchical clustering of significant gene changes across all experimental treatments. Genes downregulated are indicated in blue, whereas those upregulated are indicated in red

Selective inhibition of Aurora A induced a small accumulation of 4n cells, indicative of mitotic delay, but did not result in polyploidy and had little effect on cell cycle distribution overall (Figure 2a and b). Little cell death ($\sim$15%) was observed over this time period as indicated by FACS (Figure 2a and b) and Trypan blue exclusion (Figure 2c) despite progressive polyploidization of AZD1152- and VX-680-treated cells. We next determined the time-dependent induction of p53 under the three Aurora kinase selectivity conditions and observed that p53 was time-dependently induced following inhibition of Aurora B and A/B, but not Aurora A (Figure 2d). The induction of the cyclin-dependent kinase inhibitor p21, a canonical p53 target gene, displayed a similar pattern of regulation, indicating that p53 was active under these conditions. Moreover, when p53 short hairpin RNA (shRNA) was induced by doxycycline, the accumulation of both p53 and p21 was suppressed in the presence of AZD1152 (Figure 2e).

Upon validating the experimental model, we defined the time-dependent transcriptional response to the three pre-selected inhibitor conditions in D54MG^{shp53} in the presence or absence of doxycycline. Time-dependent modulation of the transcriptome was observed upon both Aurora B and A/B inhibition. By 72 h, approximately 2000 significant gene changes of 1.5-fold or greater were observed for both AZD1152 and VX-680 (Figure 2f). Over the 72-h time course, MLN8054 only weakly affected global transcription (Figure 2f)

despite its effects on mitotic spindle assembly (Figure 1a and c) and the concomitant mitotic delay (Figure 2a and b). Hierarchical clustering of the >2000 significant gene changes revealed that the transcriptional responses between AZD1152 and VX-680 were most correlated at each time point (Figure 2g). In cells treated with either AZD1152 or VX-680, $\sim 50\%$ of the transcriptional response was eliminated when p53 was suppressed (Figure 2f), indicating that p53 governs the bulk of the transcriptional output during polyploidization. Pathway analysis of p53-dependent genes revealed a strong bias for gene ontologies involved in cell cycle control, including G1/S transition, DNA replication, recombination, repair, synthesis, and G2/M transition. This ensemble of cell cycle regulatory genes was collectively repressed during polyploidization when p53 was functional (Supplementary Figure S1A) and not regulated when p53 was knocked down (Supplementary Figure S1B; Supplementary Table S1). Cell cycle suppression was further confirmed using two markers of cell cycle progression, phosphorylation of Rb and Cdc2, which showed p53-dependent inhibition at the 72-h time point (Figure 3a).

As p53 is inactivated in a significant proportion of human gliomas, we performed a second analysis, biased for p53-independent gene regulation, to identify candidate apoptosis-sensitizing genes that could be exploited in combination with Aurora kinase inhibitors irrespective of p53 status. This analysis was performed on the 72-h time point following exposure to AZD1152, as almost all cells have undergone endoreduplication by this point. This analysis revealed 113 apoptotic genes that were regulated as a function of Aurora B kinase inhibition with little or no influence of p53 status (Supplementary Figure S1C–D and Supplementary Table S2). Of these, TRAIL-R2/DR5 (TNFRSF10B) was of particular interest, as therapeutic agonists of this death receptor have been shown to possess both broad antitumor activity and desirable therapeutic window in preclinical models,[12–17] including glioma.[18,19] Immunoblot analysis of AZD1152-treated D54MG^{shp53} cell lysates over a 72-h time course showed that induction of TRAIL-R2 at the protein level is partially p53-dependent, although at 72 h post-treatment, the contribution of p53 is reduced (Figure 3b), presumably because of the activity of additional stress pathways that enforce TRAIL-R2 expression during polyploidization. We did not detect a change in expression of the other major TRAIL receptor, TRAIL-R1 (Figure 3b). We also observed upregulation of Noxa and downregulation of Mcl-1 at the 72-h time point (Figure 3b), which might be predicted to potentiate various apoptotic stimuli that ultimately converge on the mitochondrial apoptotic pathway. We observed a time-dependent increase in TRAIL-R2 expression on the cell surface after inhibition of

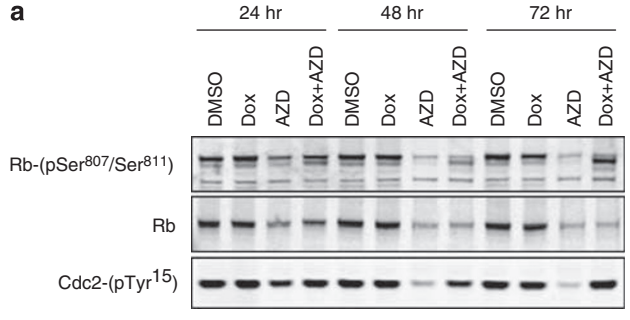

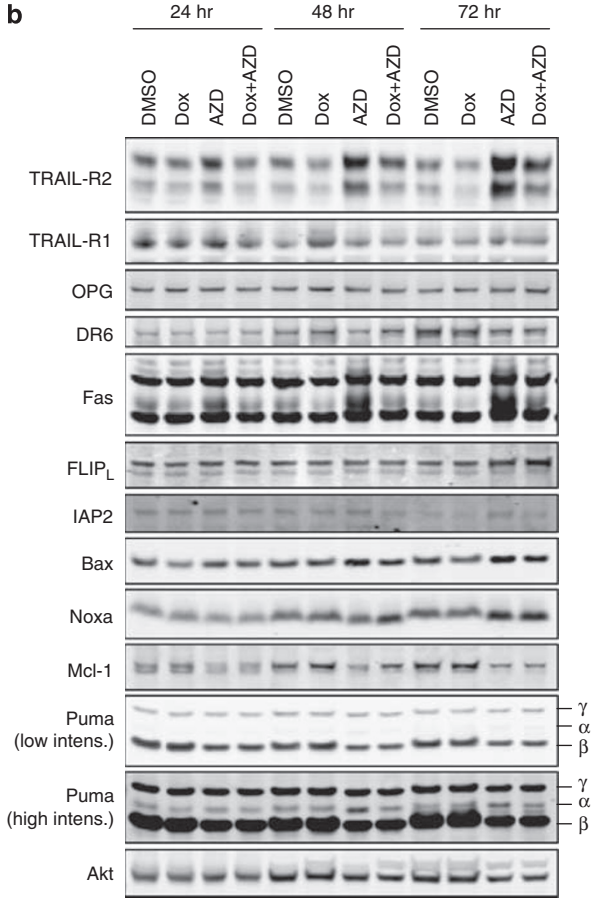

Figure 3 Continued.

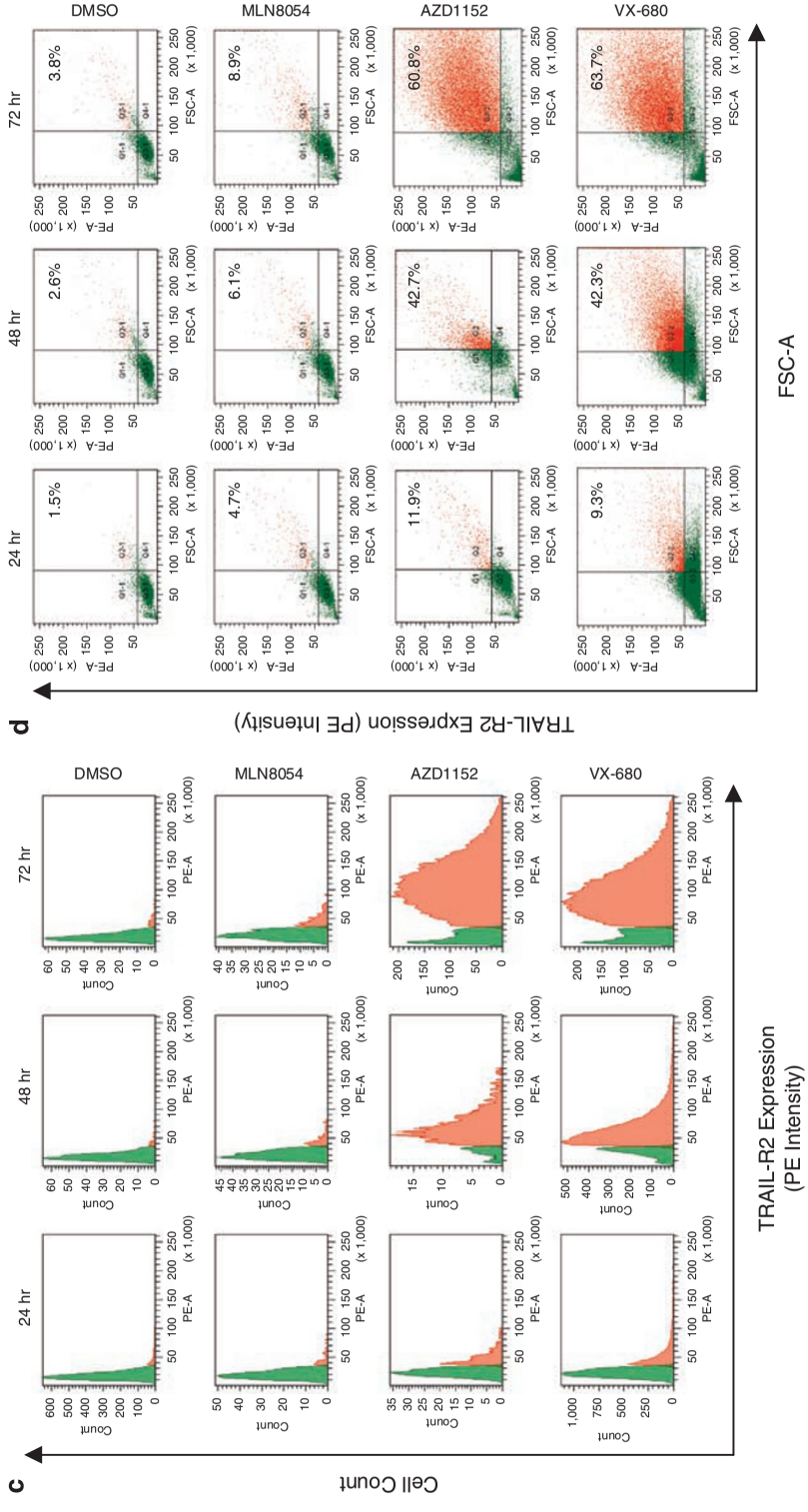

Figure 3 Modulation of TRAIL-R2 and accessory apoptotic pathway components during polyploidization. (**a**) D54MG^{shp53} cells were treated with 50 ng/ml doxycycline for 24 h prior to the addition for 200 nM AZD1152 for the times indicated. Cell lysates were then prepared, and Rb and Cdc2 phosphorylation was determined by immunoblotting. (**b**) Immunoblot analysis of various apoptotic proteins whose corresponding gene displayed some transcriptional regulation by microarray after exposure to 200 nM AZD1152 for 72 h in the presence or absence of 50 ng/ml doxycycline. (**c** and **d**) D54MG^{shp53} cells were treated with DMSO, 250 nM MLN8054, 200 nM AZD1152, or 1000 nM VX-680 and cultured for a further 24, 48, or 72 h as indicated. Cells were detached, washed, and stained with PE-labeled anti-TRAIL-R2 antibody. PE intensity was then quantified by flow cytometry and expressed as a function of cell number (**c**) or cell size (FSC-A; **d**). The populations shown in green represent basal TRAIL-R2 expression and were defined by gating the entire cell population following DMSO treatment. Population of cells that exhibit increased TRAIL-R2 expression is shown in orange. In (**d**), the percentages indicate the proportion of cells in the population that show both increased FSC-A and PE staining

Aurora B or A/B, but not Aurora A (Figure 3c), which was a function of cell size (a surrogate marker for polyploidization; Figure 3d), suggesting that cell surface expression of TRAIL-R2 and polyploidization are phenotypically coupled. Using CD44 as a marker for cell surface area, we noted that the stainable surface of D54MG^{shp53} cells increases 3.8-fold after 72 h of polyploidization, consistent with the overall increase in cell size (Supplementary Figure S2). Surface staining of TRAIL-R2 and OPG were increased 7.5- and 5-fold, respectively, 72 h after the addition of AZD1152 (Supplementary Figure S2). TRAIL-R1 expression was similar to that of CD44 and increased 3.8-fold (Supplementary Figure S2), indicating that it was not induced on a per cell basis, but rather the increased staining reflects the increase in surface area that accompanies polyploidization.

Given that induction of TRAIL-R2 by chemotherapeutics sensitizes glioma cells to TRAIL-mediated apoptosis,[20] we postulated that polyploidization may also be a TRAIL-sensitizing process. We tested this hypothesis directly by determining first whether or not TRAIL would cooperate with Aurora kinase inhibitors to suppress cell proliferation. When assayed for effects on 72-h proliferation, AZD1152 and VX-680 typically produce approximately 30–50% inhibition in D54MG^{shp53}. As noted earlier (Figure 2c), cell death during this period is minimal. By time-lapse video microscopy, we have determined that length of the D54MG^{shp53} cell cycle is extended approximately twofold during the first 72 h of polyploidization (data not shown), consistent with microarray data indicating global suppression of cell cycle-regulated processes (Supplementary Figure S1A and B). Thus, the inhibition of 72-h proliferation obtained with Aurora B- or A/B-selective treatments (i.e., AZD1152 or VX-680, respectively) reflects the combination of cell cycle suppression and loss of viability. When treated with any of the three Aurora kinase inhibitors at concentrations sufficient to inhibit Aurora B (see Figure 1c), D54MG^{shp53} cells responded to TRAIL concentrations (0.78–3.13 ng/ml) below those required to elicit an antiproliferative response (Figure 4a–c). Moreover, while in a 72-h assay, Aurora B inhibition resulted in ~50% inhibition of cell proliferation, when combined with TRAIL, close to 100% inhibition was achieved at concentrations of TRAIL (~6.25 ng/ml) that alone only produce ~20% inhibition. Inhibition of Aurora B was consistently synergistic with TRAIL within the range of 3.13–6.25 ng/ml as determined using the Bliss additivism model (Figure 4d–f). We confirmed that the inhibition of proliferation observed by the addition of TRAIL

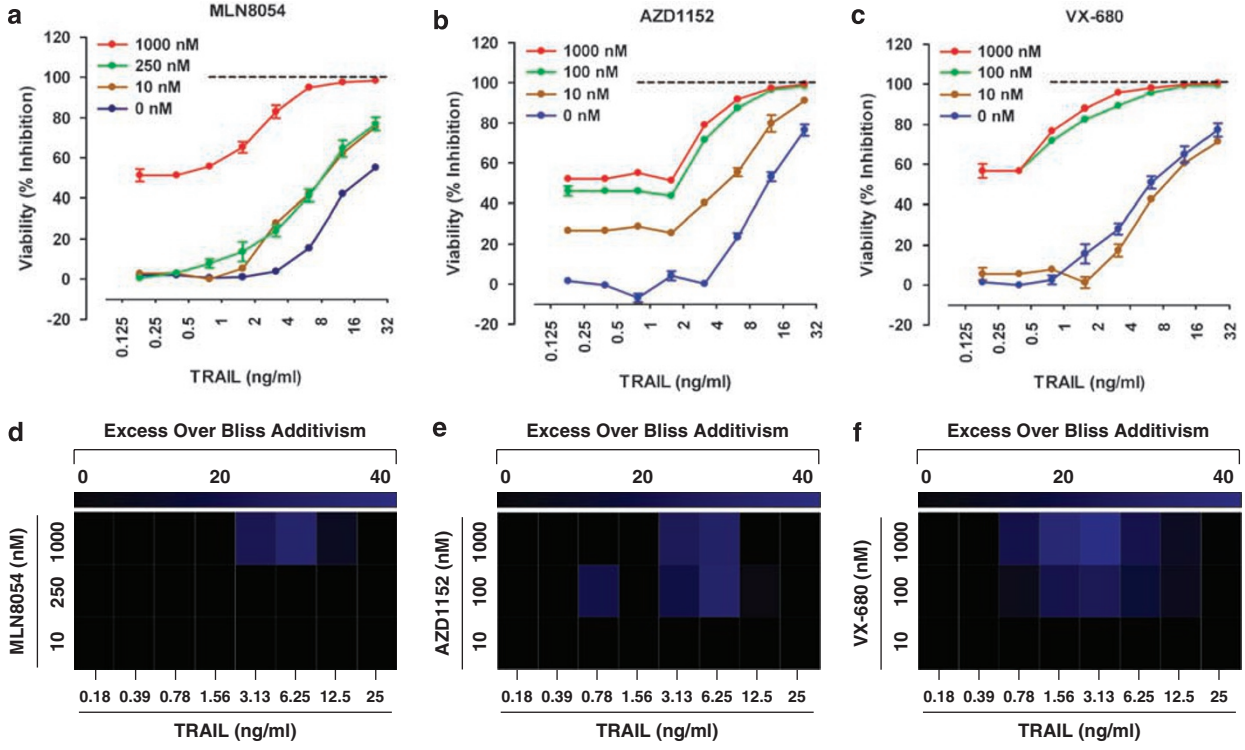

Figure 4 Aurora B kinase inhibition sensitizes glioma cells to the antiproliferative effects of TRAIL. D54MG^{shp53} cells were simultaneously treated with multiple fixed concentrations of MLN8054 (**a**), AZD1152 (**b**), and VX-680 (**c**) in combination with twofold dose responses of recombinant human TRAIL for a period of 72 h. Cell viability was then determined and expressed as a percentage of DMSO-treated controls without TRAIL. Dashed lines indicate 100% loss of viability. (**d–f**) Bliss Independence was determined for each TRAIL dose response in combination with the respective fixed concentrations of Aurora inhibitor. Scores >20 in excess of the predicted value for Bliss additivism (shown in blue) was used to define synergistic activity between both agents. These scores are expressed in heat map format. (**g**) D54MG^{shp53} cells were simultaneously exposed to 250 nM MLN8054, 200 nM AZD1152, or 1000 nM VX-680 and TRAIL in twofold dose response for 48 h. After this period, the enzymatic activity of caspase-3/-7 was determined and the data WERE expressed as fold change over DMSO-treated controls receiving no TRAIL. (**h**) D54MG^{shp53} cells were treated for 72 h with AZD1152 before the addition of 50 ng/ml TRAIL for the times indicated. Cell lysates were then prepared and immunoblotted for components of the extrinsic apoptotic pathway as indicated. (**i**) A172 cells were treated for 72 h with 200 nM AZD1152, then lysates were prepared and immunoblotted. (**j**) A172 cells were treated as described in (**b**), and cell viability was determined after 72 h. (**k**) Bliss Independence was determined and expressed was as detailed in (**d–f**)

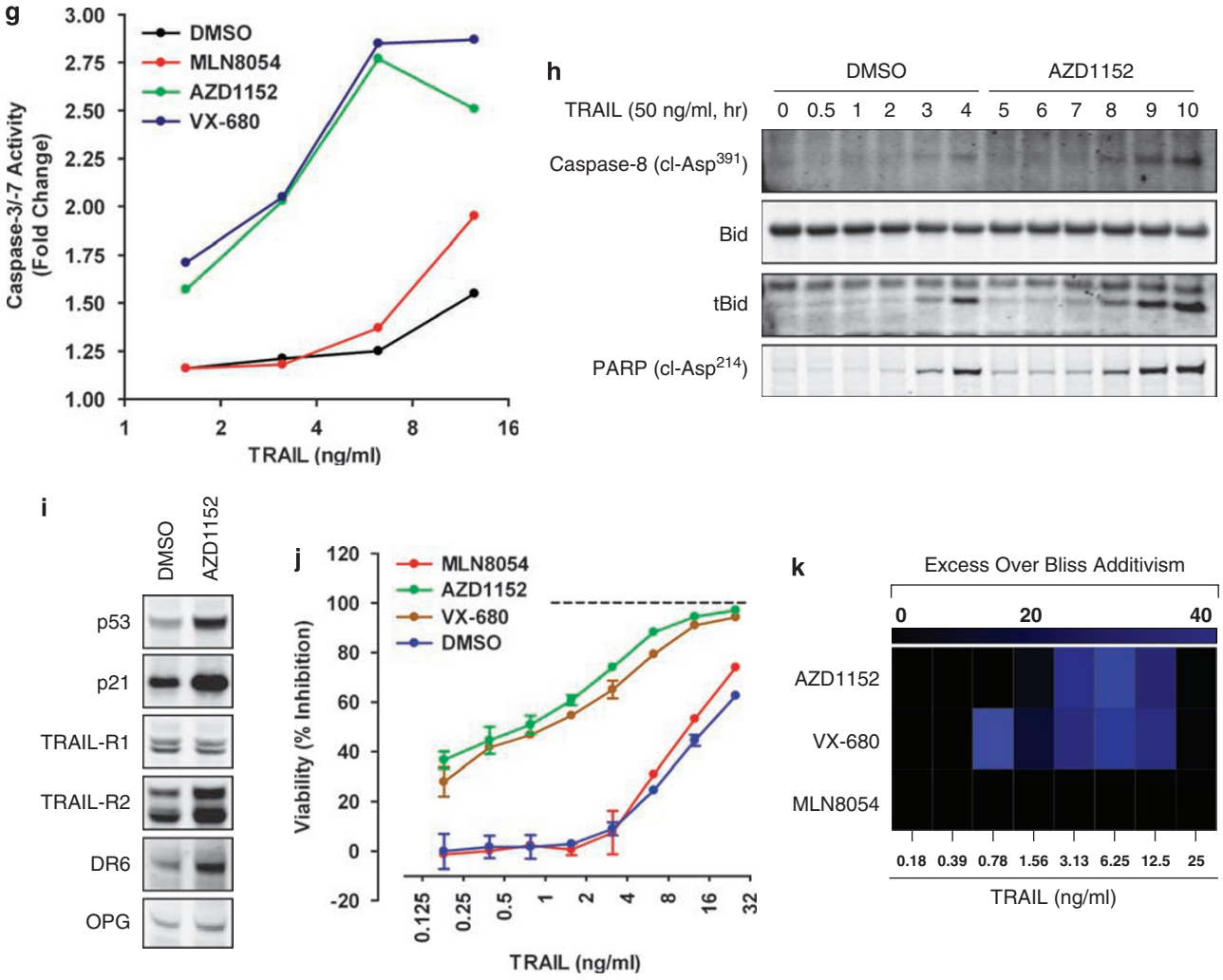

Figure 4 Continued.

was due to apoptosis, as the enzymatic activity of caspase-3 was synergistically enhanced in the presence of Aurora A/B or B inhibition, but not with inhibition of Aurora A (Figure 4g). Furthermore, exposure to TRAIL resulted in the appearance of cleaved caspase-8, tBid, and PARP, which were collectively augmented following polyploidization (Figure 4h). Altogether, these data indicated that hypersensitivity to TRAIL in D54MG^{shp53} was secondary to inhibition of Aurora B-mediated polyploidization. A172 glioma cells displayed a similar induction of TRAIL-R2 following Aurora B inhibition (Figure 4i) and exhibited a similar sensitization to recombinant TRAIL when combined with Aurora B or A/B inhibition, but not with inhibition of Aurora A (Figure 4j–k).

We attempted to assess how general polyploidy-mediated TRAIL hypersensitization was across human glioma cell lines while simultaneously addressing two significant issues: (1) to what degree was this influenced by p53 status, and (2) does polyploidization resensitize a cell line that is otherwise insensitive to TRAIL-induced apoptosis? In our evaluation of three additional cell culture models of glioblastoma multiforme (Supplementary Figure S3A–C), the combination of AZD1152 or VX-680 and TRAIL was less than additively antiproliferative in LN18 (p53^{Mut}), whereas U87MG (p53^{WT}) and U138MG (p53^{Mut}) failed to show hypersensitivity to TRAIL when combined with Aurora kinase inhibition. Immunoblot analysis of several components of the cell-extrinsic apoptosis machinery identified in our microarray analysis (Supplementary Figure S3D) revealed a lack of induction of TRAIL-R2 by AZD1152 in these lines, indicating that TRAIL-R2 induction is a correlate of TRAIL sensitivity. We also noted that, in LN18, U87MG, and U138MG, which were less sensitive to TRAIL, osteoprotegerin (OPG), a TRAIL decoy receptor, was comparatively overexpressed (Supplementary Figure S3D), potentially contributing to the enhanced resistance to TRAIL observed for these cell lines.

If TRAIL-R2 was indeed required to hypersensitize polyploid cells to TRAIL, siRNA-mediated depletion of TRAIL-R2 should either reduce the sensitivity to TRAIL or abolish TRAIL sensitivity altogether. We first evaluated a panel of four siRNAs for their ability to knock down TRAIL-R1 and TRAIL-R2 in the presence and absence of AZD1152 (Supplementary Figure S4A and C). Of these, siTRAIL-R1-2 (hereafter

referred to as siTRAIL-R1) and siTRAIL-R2-4 (hereafter referred to as siTRAIL-R2) were selected for subsequent studies on the basis of superior potencies. In D54MG^{shp53}, siTRAIL-R2 reduced TRAIL-R2 expression in AZD1152-treated cells below the level of TRAIL-R2 in DMSO-treated controls, (Figure 5a). In A172, TRAIL-R2 knockdown was more dramatic, approaching 100% (Figure 5a). Cleavage of caspase-8 and Bid were partially suppressed in D54MG^{shp53} transfected with siTRAIL-R2 both in the presence or absence of AZD1152 (Figure 5b). Moreover, TRAIL-R2 knockdown in AZD1152-treated D54MG^{shp53} cells restored TRAIL sensitivity to that of DMSO-treated controls transfected with a nontargeting siRNA (Figure 5c). In A172, where TRAIL-R2 knockdown was more complete, both AZD1152- and DMSO-treated cells were rendered completely insensitive to TRAIL, at the level of caspase-8 and Bid cleavage (Figure 5d) and overall proliferation (Figure 5e). In contrast, knockdown of TRAIL-R1 in D54MG^{shp53} cells did not affect TRAIL sensitivity in combination with Aurora B inhibition (Supplementary Figure S4B).

If the upregulation of TRAIL-R2 is sufficient to render polyploid cells sensitive to TRAIL, then depletion of TRAIL-R2 in AZD1152-treated cells to basal, DMSO-treated levels should mitigate sensitization to TRAIL. D54MG^{shp53} cells were transfected with siTRAIL-R2 in dose response, and the siRNA concentration range necessary to deplete TRAIL-R2 to baseline levels was defined (Figure 6a). We then determined the sensitivity of these cells to TRAIL at various TRAIL-R2 levels in an assay of cell viability. Baseline levels of TRAIL-R2 are achieved within the range of 0.01–0.1 nM siTRAIL-R2 (Figure 6a). A concentration of 0.01 nM siTRAIL-R2 suppressed the synergistic activity observed in cells treated with AZD1152 and TRAIL (Figure 6b and c), indicating that the increased surface expression of TRAIL-R2 can account for the

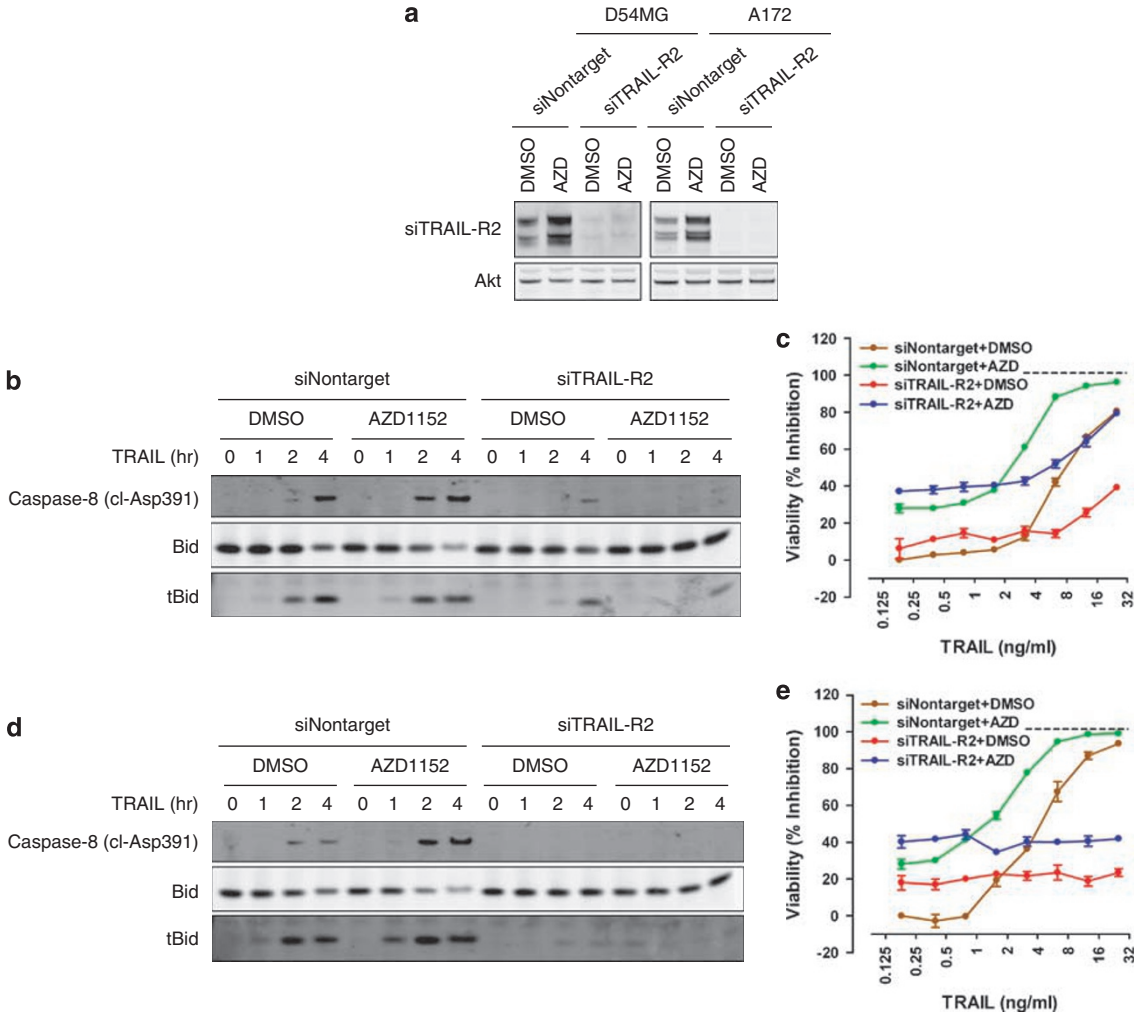

Figure 5 siRNA-mediated depletion of TRAIL-R2 rescues glioma cells from the combination of Aurora B inhibition and TRAIL. (**a**) D54MG^{shp53} and A172 cells were transfected with either siNontarget or siTRAIL-R2 (corresponds to siTRAIL-R2-4) oligos and cultured in the presence or absence of 200 nM AZD1152 for a further 72 h. Cell extracts were prepared and TRAIL-R2 knockdown was assessed by immunoblotting. D54MG^{shp53} (**b**) and A172 (**d**) cells were transfected with siNontarget or siTRAIL-R2 oligos for 48 h before the addition of 200 nM AZD1152. Cells were cultured for a further 72 h before the addition of 50 ng/ml TRAIL for the times indicated. The activation/cleavage of caspase-8 and Bid was then determined by Western blotting. D54MG^{shp53} (**c**) and A172 (**e**) cells were transfected with siNontarget or siTRAIL-R2 oligos for 48 h before the simultaneous addition of 200 nM AZD1152 and TRAIL in twofold dose response. Cells were cultured for a further 72 h, and cell viability was determined

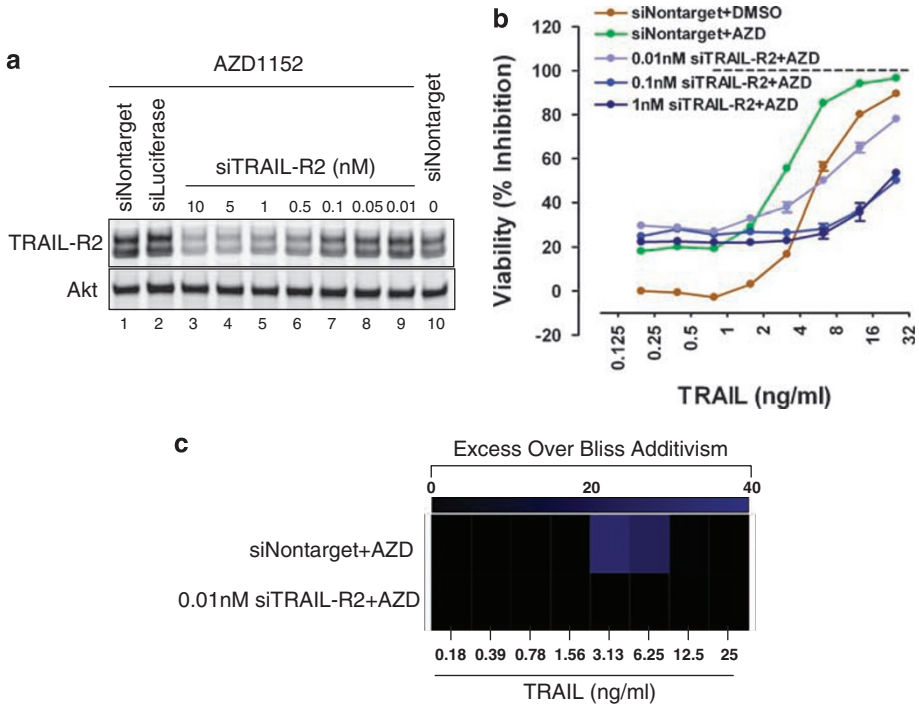

Figure 6 Increased expression of TRAIL-R2 is sufficient to sensitize glioma cells to TRAIL following inhibition of Aurora B. (**a**) D54MG^{shp53} cells were treated siTRAIL-R2 in dose response for 48 h, then treated with 200 nM AZD1152 for an additional 72 h. Lysates were prepared and immunoblotted to compare basal levels of TRAIL-R2 (lane 10) to AZD1152-induced levels over the siTRAIL-R2 dose response (lanes 1–9). TRAIL-R2 was reduced to basal levels at siRNA concentrations between 0.01 and 0.1 nM siTRAIL-R2. (**b**) D54MG^{shp53} cells were treated as indicated in (**a**) and cell viability was determined. (**c**) Bliss Independence analysis of (**b**) demonstrates that synergistic activity observed for AZD1152 and TRAIL is lost when TRAIL-R2 is depleted to basal, untreated levels

sensitization to TRAIL upon Aurora B inhibition observed in this model.

Discussion

Our data reveal that the transcriptional response to inhibition of Aurora B is virtually indistinguishable from the response elicited when Aurora A and B are simultaneously repressed, suggesting that Aurora B inhibition is the dominant activity in this context. The Aurora A-selective agent, MLN8054, has been shown to induce apoptosis in multiple cancer cell lines and display antitumor activity *in vivo*.[3] However, owing to its dual specificity at higher concentrations, it has been difficult to reconcile whether this truly reflects inhibition of Aurora A or the combined activities of Aurora A and B. At 250 nM, a concentration of MLN8054 that almost completely suppresses mitotic spindle assembly although negligibly affecting mitotic histone H3 phosphorylation (Figure 1), we observed a striking lack of transcriptional response despite a modest accumulation of cells with 4n DNA content (Figure 2a and b). This was an unexpected observation, as depletion of Aurora A with siRNA has been shown to be antiproliferative in multiple pancreatic cancer cell lines.[1,21] These seemingly discrepant results could suggest a phenotypic difference between small molecule-based inhibition of Aurora A kinase and depletion of the protein or reflect lineage-specific susceptibilities to Aurora A inhibition.

Our data shed new light on the transcriptional processes modulated during polyploidization and highlight the involvement of p53. It has been appreciated for some time that polyploidization resulting from cytokinesis failure engages p53,[10] limiting further endoreduplication and thus further polyploidization as a result of cell cycle suppression.[9] After cytokinesis failure, cancer cells lacking functional p53 proceed in an unrestrained manner through the cell cycle, rapidly undergoing successive rounds of polyploidization, which eventually induces apoptosis.[11] And so, temporarily (and perhaps paradoxically), the cell cycle-suppressive effects of p53 appear to maintain cell viability during polyploidization, although most cells with wild-type p53 will also eventually succumb to this process (data not shown).

Additionally, p53 participates in programmed cell death on multiple levels, both as a transcriptional regulator of extrinsic and intrinsic apoptotic pathway genes and, as uncovered more recently, by directly activating the proapoptotic factor, Bax.[22] Our data indicate that following cytokinesis failure, the chief function of p53 is to orchestrate multiple processes involved in cell cycle suppression rather than triggering rapid and overt apoptosis because during the first 72 h of polyploidization, little cell death is observed (Figure 2c). Our data suggest that polyploidization lowers the threshold for apoptosis by upregulating and priming the apoptotic machinery. This program comprises elements of both the cell-intrinsic and -extrinsic apoptotic pathways, where it is ultimately the balance of pro- and anti-apoptotic factors that determine the sensitivity to further apoptotic insult. With regard to the latter, the upregulation of TRAIL-R2 observed during

polyploidization represents a potential point of therapeutic intervention. Although a correlation between death receptor upregulation and TRAIL sensitivity is not always observed, multiple anticancer therapies that upregulate TRAIL-R1 and TRAIL-R2 also show synergistic activity when combined with rTRAIL[20,23–26] or agonistic death receptor antibodies.[27,28] There is generally poor agreement between TRAIL-R2 expression in response to various pharmacological manipulations and p53 status,[29,30] suggesting that although p53 can positively regulate the expression of TRAIL-R2, alternative routes to TRAIL-R2 transcription also exist. Our data support these conclusions, as TRAIL-R2 expression is only partially attenuated after 72 h of exposure to AZD1152 in the absence of p53. We have also observed that the hypersensitivity of polyploid cells to TRAIL is only slightly blunted by p53 knockdown (data not shown). These data are aligned with earlier failures to establish a direct link between the expression of functional p53 and TRAIL sensitivity.[25,31–33]

A simplistic view is that TRAIL sensitivity reflects both cell-surface expression of TRAIL receptors and the functionality of death receptor pathway effector components. Our data suggest that, in part, the sensitization to TRAIL that occurs during polyploidization reflects the upregulation of TRAIL-R2. In both D54MG^{shp53} and A172, a substantial induction of TRAIL-R2 is observed concomitant with TRAIL hypersensitivity (*cf.* Figures 3b and 4b; *cf.* Figure 4i and j). Furthermore, in D54MG^{shp53} cells, siRNA-mediated suppression of TRAIL-R2 induces resistance to TRAIL, as higher concentrations of TRAIL are required to elicit the same antiproliferative effect. In fact, the TRAIL dose response curve of AZD1152-treated cells after TRAIL-R2 knockdown is similar to control, DMSO-treated cells (Figure 6b). In A172, knockdown of TRAIL-R2 renders both normal and polyploid cells completely refractory to TRAIL (Figure 6d). The differential effect of TRAIL-R2 knockdown on TRAIL sensitivity in D54MG^{shp53} and A172 correlates well with the extent of TRAIL-R2 suppression (Figure 5d). These data also suggest that TRAIL-R2, rather than other TRAIL receptors, such as TRAIL-R1, is the primary receptor contributing to TRAIL sensitivity when combined with inhibition of Aurora B. An additive antiproliferative effect of combining TRAIL and AZD1152 is observed in LN18 (Supplementary Figure S3A), although this does not involve TRAIL hypersensitivity *per se* as both DMSO- and AZD1152-treated cells respond to similar concentrations of TRAIL. Whereas LN18, U87MG, and U138MG display comparatively low expression of TRAIL-R2, TRAIL-R1 expression is somewhat elevated in LN18 (Supplementary Figure S3D), which could explain its intermediate response. Both U87MG and U138MG were completely insensitive to TRAIL concentrations below 25 ng/ml (Supplementary Figure S3B and C). Although OPG has been most extensively studied as a decoy receptor for soluble RANKL,[34] its analogous role as a TRAIL decoy receptor is also appreciated, as soluble OPG protects multiple cancer cell lines from apoptosis induced by TRAIL.[35] It is also potentially significant that LN18, U87MG, and U138MG expressed comparatively high levels of OPG, which could also contribute to overall TRAIL resistance. Nevertheless, in these glioma cell lines, polyploidization does not appear to sensitize an otherwise TRAIL-resistant cell line to the apoptotic effects of TRAIL.

Although activating the cell-extrinsic apoptotic pathway as a means of inducing cancer cell apoptosis is a concept that has been appreciated for some time, the preferential cytotoxicity of TRAIL for transformed *versus* normal cells has, to date, translated into a meaningful therapeutic window in preclinical models, as recombinant TRAIL is both efficacious in human tumor xenografts and systemically well tolerated.[12,13] Agonistic anti-TRAIL-R1 or -TRAIL-R2 antibodies also display promising antitumor activity in human xenograft models without overt systemic toxicity.[14–17] As many chemotherapeutics induce TRAIL-R1/-R2, considerable attention has been given to therapeutic strategies that combine these agents with TRAIL or TRAIL-R1/-R2 agonistic antibodies. In individuals with glioblastoma mulitforme, expression of TRAIL-R1 and TRAIL-R2 are independent prognostic indicators of patient survival,[36] suggesting that these death receptors play an active role in tumor suppression in this setting. Our data show that pharmacological inhibition of Aurora B induces TRAIL-R2 concomitant with TRAIL sensitization in a subset of human glioma cell lines secondary to polyploidization and further suggest that inhibition of Aurora B may be an effective means to sensitize glioblastoma multiforme to TRAIL-mediated apoptosis.

Materials and Methods

Cell culture. To create the D54MG^{shp53} cells, 2O2-shRNA(p53), a plasmid designed to express an shRNA (gacuccagugguaaucuacucucuugaa guagauuaccacuggagucuu) against p53 under the control of a tet-responsive U6 promoter, was introduced into the previously described D54MG-tetR cells.[37] Stable clones that exhibited doxycycline-dependent ablation of the p53 protein were identified and designated as D54MG^{shp53} A172, LN18, U87MG, and U138MG glioma cells and were purchased from American Type Culture Collection and propagated as recommended. D54MG^{shp53} cells were cultured in DMEM without sodium pyruvate supplemented with 10% Tet-approved FBS (v/v), 0.1 mM nonessential amino acids, and penicillin/streptomycin.

Reagents. Recombinant human TRAIL was purchased from Sigma. The chemical structures of MLN8054 (4-{[9-choloro-7-(2,6-difluorophenyl)-5*H*-pyrimido[5,4-D][2]benzazepin-2-yl]amino}-benzoic acid),[3] AZD1152 (2-[[3-({4-[(5-{2-[(3-Fluorophenyl)amino]-2-oxoethyl}-1*H*-pyrazol-3-yl)amino]-quinazolin-7-yl}oxy) propyl](ethyl)amino]ethyl dihydrogen phosphate),[5] and VX-680/MK-0457 (cyclopropane carboxylic acid {4-[4-(4-methyl-piperazin-1-yl)-6-(5-methyl-2H-pyrazol-3-ylamino)-pyrimidin-2-ylsulphanyl]-phenyl}-amide)[7] have been disclosed. These compounds were synthesized at Abbott Laboratories for comparative purposes. AZD1152-hydroxyquinazoline pyrazol anilide (HQPA) is rapidly converted from the dihydrogen phosphate prodrug, AZD1152, in the presence of plasma.[5] For all relevant studies, AZD1152-HQPA was used and hereafter referred to as AZD1152. Antibodies were purchased as follows: TRAIL-R2, FLIP, IAP2, cleaved caspase-8 (Asp^{391}), Puma, and Cy5-conjugated MPM-2 was purchased from Cell Signaling Technology; p53, OPG, Bid, and cleaved PARP (Asp^{214}) were purchased from BD Biosciences; p21 was purchased from Upstate Biotechnology; Bax, TRAIL-R1, and DR6 were purchased from Abcam; and Fas was purchased from Santa Cruz Biotechnology. Phycoerythrin (PE)-conjugated anti-human TRAIL-R1, TRAIL-R2, and OPG antibodies were purchased from R&D systems and Axxora. PE-conjugated anti-CD44 antibody was obtained from BD Biosciences. Histone H3-(pSer^{10}) antibodies were obtained from Cell Signaling Technology and Upstate Biotechnology. Antibodies for α-tubulin were obtained from Abcam And Hoechst DNA stain was obtained from Molecular Probes.

Immunofluorescence. D54MG^{shp53} cells were plated on 8-well chamber slides (Lab-Tek II) at 30 000/well in 0.3 ml of growth medium. Cells were treated the following day for 6 h with compounds as indicated at 10, 3, 1, 0.3, 0.1, 0.03, 0.01, and 0 μM on two slides each by adding 33 μl of half-log, serially diluted compound. Slides were washed once with 1 ml of PBS, then fixed in 0.2 ml of methanol/acetone (1 : 1) for 5 min at room temperature. Slides were washed four times with 1 ml of

PBS, then blocked with 5% goat serum in PBS for 2 h. Fixed cells were incubated overnight at 4°C with primary antibody diluted in blocking buffer. Slides were then washed three times in 1 ml of PBS and incubated for 2 h at room temperature with anti-rabbit Alexa Fluor 488 (Molecular Probes) diluted in blocking buffer. Slides were washed three times with 1 ml of PBS, stained with Hoechst DNA stain (Molecular Probes) in PBS for 5 min, then washed once with 1 ml PBS. Chambers were removed, and the slides were dried and mounted with ProlongGold (Molecular Probes) and coverslips. The cells were examined and imaged under a fluorescent microscope.

Flow cytometry. To monitor cell cycle distribution and polyploidization, D54MG^{shp53} cells were treated as indicated and then washed with PBS, detached, and resuspended in PBS containing 50 μg/ml propidium iodide, 0.1% Triton X-100, and 50 U RNase. Cells were incubated for 1 h at 37°C and DNA content was determined using a BD LSR II flow cytometer (BD Biosciences). To determine cell surface expression of CD44, TRAIL-R1, TRAIL-R2, and OPG, cells were treated, washed, detached, washed again, and incubated in the presence of PE-conjugated anti-CD44, anti-TRAIL-R1, or anti-TRAIL-R2 antibody for 45 min on ice. PE intensity was then determined by flow cytometry.

Trypan blue exclusion. Cell viability was determined on cells present both in the culture medium and attached to plates. Briefly, the culture medium was collected and centrifuged to pellet any detached cells. Cells that remained adherent were washed in PBS, detached, and combined with the cellular fraction initially prepared from the culture medium and Trypan blue exclusion performed using a Vi-CELL cell counter (Beckman Coulter).

Gene expression analysis by microarray. Cell samples were lysed and total RNA was isolated using the QIAshredder and RNeasy columns (Qiagen). Labeled cRNA was prepared according to the microarray manufacturer's protocol and hybridized to human genome U133A 2.0 arrays (Affymetrix). The microarray data files were loaded into Rosetta Resolver software for analysis, and the intensity values for all probesets were normalized using the Resolver's Experimental Definition. Clustering analysis within Resolver used the Agglomerative algorithm and Pearson correlation for the similarity measure, using genes that had a 1.5-fold change or higher in 1 treatment condition. Only differences with a *P*-value less than 0.001 are shown in color. For the pathway analysis, a 1.5-fold cutoff was applied and a 5% false discovery rate was used for *P*-value cutoff.[38]

Pathway analysis and *in silico* construction of biological networks. Pathway analysis of whole genome microarray data was performed using Ingenuity Pathway Analysis (IPA; Ingenuity Systems) software. Only gene expression data that satisfied both the *P*-value significance cutoff were analyzed. To determine p53-dependent transcriptional networks, a D54MG^{shp53} gene list comparison was made between two treatment conditions: (1) AZD1152 (200 nM, 72 h) without dox *versus* (2) AZD1152 (200 nM, 72 h) with dox. By subtractive comparison, the gene set unique to the first condition comprised the p53-dependent gene list. This list was then uploaded into IPA and a core analysis was performed to empirically identify significantly modulated gene ontologies. Individual subnetworks associated with G1/S transition, S phase, DNA replication, recombination, repair, and G2/M checkpoints were then grown and combined to construct a comprehensive network comprising significantly modulated cell cycle control genes. Once the pathway was constructed, the parent microarray data sets from AZD1152 (200 nM, 72 h) without dox and AZD1152 (200 nM, 72 h) with dox were applied to the network. A p53-independent transcriptional network was constructed similarly, first by comparing the two aforementioned gene lists obtained from D54MG^{shp53}: (1) AZD1152 (200 nM, 72 h) without dox *versus* (2) AZD1152 (200 nM, 72 h) with dox. The common gene set, which was not influenced by p53 status, defined the p53-independent gene list. A core analysis was performed on this data set, and subnetworks associated with the apoptosis gene ontology were grown and connected to generate a larger network of apoptosis genes significantly regulated under this treatment condition. Again, once the pathway was constructed, the parent data sets from AZD1152 (200 nM, 72 h) without dox and AZD1152 (200 nM, 72 h) with dox were applied.

Cell proliferation assay. Cells were seeded into 96-well plates at 2500/well and allowed to adhere overnight. Compounds and TRAIL were added the following day, and cells were incubated at 37°C for a further 72 h. Inhibition of cell proliferation was determined using CellTiter-Glo Luminescence Cell Viability Assay (Promega) as suggested by the manufacturer and luminescence was quantified using a SpectraMax M5^e plate reader (Molecular Devices). Percentage of inhibition of viability was determined relative to cells treated with DMSO alone (0.1%). Data are representative of at least three independent experiments with each data point carried out in triplicate.

Caspase-3 activity assay. Cells were seeded into 96-well plates at 10 000/well and allowed to adhere overnight. Compounds and TRAIL were added the following day, and cells were incubated at 37°C for 48 h. The activity of caspase-3/-7 was measured using Caspase-Glo 3/7 Assay (Promega) as suggested by the manufacturer and luminescence was quantified using a SpectraMax M5^e plate reader (Molecular Devices).

siRNA-mediated knockdown of TRAIL-R1 and TRAIL-R2. A total of 50 000 cells/well were transfected in 24-well plates in the absence of antibiotics with one of the following siRNA oligos (Dharmacon) using Lipofectamine RNAiMAX transfection reagent (Invitrogen) according to the manufacturer's instructions: nontargeting siRNA (cat. no. D-001810-01), siTRAIL-R1-1 (cat. no. J-008090-07), siTRAIL-R1-2 (cat. no. J-J-008090-08), siTRAIL-R1-3 (cat. no. J-008090-09), siTRAIL-R1-4 (cat. no. J-008090-10), siTRAIL-R2-1 (cat. no. J-004448-05), siTRAIL-R2-2 (cat. no. J-004448-06), siTRAIL-R2-3 (cat. no. J-004448-07), siTRAIL-R2-4 (cat. no. J-004448-08). TRAIL-R1 and TRAIL-R2 knockdown was determined after 72 h by immunoblot analysis.

To evaluate the effect of TRAIL-R1 and TRAIL-R2 knockdown on cell proliferation in the presence of the combination of AZD1152 and TRAIL, cells were seeded into 96-well plates at 5000/well in normal growth medium without antibiotics. Cells were then transfected with a control, nontargeting siRNA oligo, siTRAIL-R1-2, or siTRAIL-R2-4 siRNA at a final siRNA concentration of 10-20 nM unless otherwise stated using Lipofectamine RNAiMAX transfection reagent (Invitrogen). Forty-eight hours post-transfection, the growth medium was removed and replaced with medium containing either DMSO (0.1%) and TRAIL in dose response or AZD1152 (200 nM) and TRAIL in dose response. Cells were incubated for a further 72 h, and then effects on cell proliferation were determined as outlined above.

Statistical analysis. Synergistic activities of Aurora kinase inhibitors and recombinant TRAIL were determined using the Bliss additivism model[39] where the combined response C of both agents with individual effects A and B is $C = A + B - (A \cdot B)$ where A and B represent the fractional inhibition between 0 and 1. Combined response scores greater than 20 were considered synergistic.

Acknowledgements. We thank Zhiqin Ji for synthesizing MLN8054 and AZD1152 and Douglas H Steinman for the synthesis of VX-680. We also thank Zehan Chen for technical assistance with the flow cytometric studies carried out here and Joel D Leverson, Chris Tse, and Steven K Davidsen for critical review of the manuscript.

1. Hata T, Furukawa T, Sunamura M, Egawa S, Motoi F, Ohmura N *et al.* RNA interference targeting aurora kinase a suppresses tumor growth and enhances the taxane chemosensitivity in human pancreatic cancer cells. *Cancer Res* 2005; **65**: 2899–2905.
2. Hu HM, Chuang CK, Lee MJ, Tseng TC, Tang TK. Genomic organization, expression, and chromosome localization of a third aurora-related kinase gene, Aie1. *DNA Cell Biol* 2000; **19**: 679–688.
3. Manfredi MG, Ecsedy JA, Meetze KA, Balani SK, Burenkova O, Chen W *et al.* Antitumor activity of MLN8054, an orally active small-molecule inhibitor of Aurora A kinase. *Proc Natl Acad Sci USA* 2007; **104**: 4106–4111.
4. Hoar K, Chakravarty A, Rabino C, Wysong D, Bowman D, Roy N *et al.* MLN8054, a small-molecule inhibitor of Aurora A, causes spindle pole and chromosome congression defects leading to aneuploidy. *Mol Cell Biol* 2007; **27**: 4513–4525.
5. Mortlock AA, Foote KM, Heron NM, Jung FH, Pasquet G, Lohmann JJ *et al.* Discovery, synthesis, and *in vivo* activity of a new class of pyrazoloquinazolines as selective inhibitors of aurora B kinase. *J Med Chem* 2007; **50**: 2213–2224.
6. Yang J, Ikezoe T, Nishioka C, Tasaka T, Taniguchi A, Kuwayama Y *et al.* AZD1152, a novel and selective aurora B kinase inhibitor, induces growth arrest, apoptosis, and sensitization for tubulin depolymerizing agent or topoisomerase II inhibitor in human acute leukemia cells *in vitro* and *in vivo*. *Blood* 2007; **110**: 2034–2040.
7. Harrington EA, Bebbington D, Moore J, Rasmussen RK, Ajose-Adeogun AO, Nakayama T *et al.* VX-680, a potent and selective small-molecule inhibitor of the Aurora kinases, suppresses tumor growth *in vivo*. *Nat Med* 2004; **10**: 262–267.

8. Wilkinson RW, Odedra R, Heaton SP, Wedge SR, Keen NJ, Crafter C *et al.* AZD1152, a selective inhibitor of Aurora B kinase, inhibits human tumor xenograft growth by inducing apoptosis. *Clin Cancer Res* 2007; **13**: 3682–3688.
9. Minn AJ, Boise LH, Thompson CB. Expression of Bcl-xL and loss of p53 can cooperate to overcome a cell cycle checkpoint induced by mitotic spindle damage. *Genes Dev* 1996; **10**: 2621–2631.
10. Cross SM, Sanchez CA, Morgan CA, Schimke MK, Ramel S, Idzerda RL *et al.* A p53-dependent mouse spindle checkpoint. *Science* 1995; **267**: 1353–1356.
11. Gizatullin F, Yao Y, Kung V, Harding MW, Loda M, Shapiro GI. The Aurora kinase inhibitor VX-680 induces endoreduplication and apoptosis preferentially in cells with compromised p53-dependent postmitotic checkpoint function. *Cancer Res* 2006; **66**: 7668–7677.
12. Ashkenazi A, Pai RC, Fong S, Leung S, Lawrence DA, Marsters SA *et al.* Safety and antitumor activity of recombinant soluble Apo2 ligand. *J Clin Invest* 1999; **104**: 155–162.
13. Walczak H, Miller RE, Ariail K, Gliniak B, Griffith TS, Kubin M *et al.* Tumoricidal activity of tumor necrosis factor-related apoptosis-inducing ligand *in vivo*. *Nat Med* 1999; **5**: 157–163.
14. Griffith TS, Rauch CT, Smolak PJ, Waugh JY, Boiani N, Lynch DH *et al.* Functional analysis of TRAIL receptors using monoclonal antibodies. *J Immunol* 1999; **162**: 2597–2605.
15. Chuntharapai A, Dodge K, Grimmer K, Schroeder K, Marsters SA, Koeppen H *et al.* Isotype-dependent inhibition of tumor growth *in vivo* by monoclonal antibodies to death receptor 4. *J Immunol* 2001; **166**: 4891–4898.
16. Ichikawa K, Liu W, Zhao L, Wang Z, Liu D, Ohtsuka T *et al.* Tumoricidal activity of a novel anti-human DR5 monoclonal antibody without hepatocyte cytotoxicity. *Nat Med* 2001; **7**: 954–960.
17. Pukac L, Kanakaraj P, Humphreys R, Alderson R, Bloom M, Sung C *et al.* HGS-ETR1, a fully human TRAIL-receptor 1 monoclonal antibody, induces cell death in multiple tumour types *in vitro* and *in vivo*. *Br J Cancer* 2005; **92**: 1430–1441.
18. Pollack IF, Erff M, Ashkenazi A. Direct stimulation of apoptotic signaling by soluble Apo2 l/ tumor necrosis factor-related apoptosis-inducing ligand leads to selective killing of glioma cells. *Clin Cancer Res* 2001; **7**: 1362–1369.
19. Roth W, Isenmann S, Naumann U, Kügler S, Bähr M, Dichgans J *et al.* Locoregional Apo2L/TRAIL eradicates intracranial human malignant glioma xenografts in athymic mice in the absence of neurotoxicity. *Biochem Biophys Res Commun* 1999; **256**: 479–483.
20. Nagane M, Pan G, Weddle JJ, Dixit VM, Cavenee WK, Huang HJ. Increased death receptor 5 expression by chemotherapeutic agents in human gliomas causes synergistic cytotoxicity with tumor necrosis factor-related apoptosis-inducing ligand *in vitro* and *in vivo*. *Cancer Res* 2000; **60**: 847–853.
21. Warner SL, Munoz RM, Stafford P, Koller E, Hurley LH, Von Hoff DD *et al.* Comparing Aurora A and Aurora B as molecular targets for growth inhibition of pancreatic cancer cells. *Mol Cancer Ther* 2006; **5**: 2450–2458.
22. Chipuk JE, Kuwana T, Bouchier-Hayes L, Droin NM, Newmeyer DD, Schuler M *et al.* Direct activation of Bax by p53 mediates mitochondrial membrane permeabilization and apoptosis. *Science* 2004; **303**: 1010–1014.
23. Chinnaiyan AM, Prasad U, Shankar S, Hamstra DA, Shanaiah M, Chenevert TL *et al.* Combined effect of tumor necrosis factor-related apoptosis-inducing ligand and ionizing radiation in breast cancer therapy. *Proc Natl Acad Sci USA* 2000; **97**: 1754–1759.
24. LeBlanc H, Lawrence DA, Varfolomeev E, Totpal K, Morlan J, Schow P *et al.* Tumor-cell resistance to death receptor – induced apoptosis through mutational inactivation of the proapoptotic Bcl-2 homolog Bax. *Nat Med* 2002; **8**: 274–281.
25. Wen J, Ramadevi N, Nguyen D, Perkins C, Worthington E, Bhalla K. Antileukemic drugs increase death receptor 5 levels and enhance Apo-2L-induced apoptosis of human acute leukemia cells. *Blood* 2000; **96**: 3900–3906.
26. Nimmanapalli R, Perkins CL, Orlando M, O'Bryan E, Nguyen D, Bhalla KN. Pretreatment with paclitaxel enhances apo-2 ligand/tumor necrosis factor-related apoptosis-inducing ligand-induced apoptosis of prostate cancer cells by inducing death receptors 4 and 5 protein levels. *Cancer Res* 2001; **61**: 759–763.
27. Buchsbaum DJ, Zhou T, Grizzle WE, Oliver PG, Hammond CJ, Zhang S *et al.* Antitumor efficacy of TRA-8 anti-DR5 monoclonal antibody alone or in combination with chemotherapy and/or radiation therapy in a human breast cancer model. *Clin Cancer Res* 2003; **9**: 3731–3741.
28. Ohtsuka T, Buchsbaum DJ, Oliver PG, Makhija S, Kimberly RP, Zhou T. Synergistic induction of tumor cell apoptosis by death receptor antibody and chemotherapy agent through JNK/p38 and mitochondrial death pathway. *Oncogene* 2003; **22**: 2034–2044.
29. Meng RD, El-Deiry WS. p53-independent upregulation of KILLER/DR5 TRAIL receptor expression by glucocorticoids and interferon-gamma. *Exp Cell Res* 2001; **262**: 154–169.
30. Shankar S, Chen X, Srivastava RK. Effects of sequential treatments with chemotherapeutic drugs followed by TRAIL on prostate cancer *in vitro* and *in vivo*. *Prostate* 2005; **62**: 165–186.
31. Sheikh MS, Burns TF, Huang Y, Wu GS, Amundson S, Brooks KS *et al.* p53-dependent and -independent regulation of the death receptor KILLER/DR5 gene expression in response to genotoxic stress and tumor necrosis factor alpha. *Cancer Res* 1998; **58**: 1593–1598.
32. Röhn TA, Wagenknecht B, Roth W, Naumann U, Gulbins E, Krammer PH *et al. CCNU-dependent potentiation of TRAIL/Apo2L-induced apoptosis in human glioma cells is p53-independent but may involve enhanced cytochrome c release. Oncogene 2001;* **20***: 4128–4137.*
33. Ravi R, Jain AJ, Schulick RD, Pham V, Prouser TS, Allen H *et al.* Elimination of hepatic metastases of colon cancer cells via p53-independent cross-talk between irinotecan and Apo2 ligand/TRAIL. *Cancer Res* 2004; **64**: 9105–9114.
34. Khosla S. Minireview: the OPG/RANKL/RANK system. *Endocrinology* 2001; **142**: 5050–5055.
35. Holen I, Shipman CM. Role of osteoprotegerin (OPG) in cancer. *Clin Sci (Lond)* 2006; **110**: 279–291.
36. Kuijlen JM, Mooij JJ, Platteel I, Hoving EW, van der Graaf WT, Span MM *et al.* TRAIL-receptor expression is an independent prognostic factor for survival in patients with a primary glioblastoma multiforme. *J Neurooncol* 2006; **78**: 161–171.
37. Lin X, Yang J, Chen J, Gunasekera A, Fesik SW, Shen Y. Development of a tightly regulated U6 promoter for shRNA expression. *FEBS Lett* 2004; **19**: 376–380.
38. Benjamini Y, Hochberg Y. Controlling the false discovery rate: a practical and powerful approach to multiple testing. *J R Statist Soc B* 1995; **57**: 289–300.
39. Berenbaum MC. Criteria for analyzing interactions between biologically active agents. *Adv Cancer Res* 1981; **35**: 269–335.

Supplementary Information accompanies the paper on Cell Death and Differentiation website (http://www.nature.com/cdd)